6th NDT in Progress 2011
International Workshop of NDT Experts, Prague, 10-12 Oct 2011

Structural Health Monitoring of Aircraft Structure by Method of Electromechanical Impedance

Vitalijs PAVELKO [1], Ilmars OZOLINSH [1], Sergejs KUZNETSOV [1], Igor PAVELKO [1]

[1] Aviation Institute of Riga Technical University, Riga, Latvia
Phone: +371 67089961, Fax: +371 67089990; e-mail: vitally_pavelko@hotmail.com, ilmars_o@inbox.lv, sergei@parks.lv, Igors.Pavelko@rtu.lv

Abstract
Problems of the electromechanical impedance (EMI) method for structural health monitoring of aircraft are analyzed. The piezoceramics transducer EMI changes were investigated experimentally at the different kinds of artificial damages. The 1-D partial model of constrained PZT is developed and validated by special test. The some generalized model of EMI of 'structural element - piezoceramics transducer' is constructed for the case when modal properties of system components are known. The example of model application for effect of crack estimation to dynamics properties and the EMI is presented and the effect of a crack in a thin sheet is estimated.

Keywords: Structural health monitoring, aircraft, electromechanical impedance, fatigue crack

1. Introduction

Concept of impedance is well known as a parameter of complex resistance. Impedance is a measure of some structure or material resistance when it is subjected by a given forced action. The are different specific types of impedance (mechanical, acoustic, electrical). If some system includes two of more different physical object, then its resistance is called as combined.

In ultrasound non-destructive inspection the concept of electromechanical impedance was used primary in [1-3]. Since this time the electromechanical impedance (EMI) several authors used the EMI method for structural health monitoring, by comparing the impedance method was used efficiently for damage detecting in different kinds of structure [4-10 and other.]. Many examples of application of EMI method can find in fundamental monographs [11,12]. The effect of structural damage is associated with the changes of dynamic properties of a structure and can be effectively defined at ultrasonic frequencies by identification of EMI of system 'sensor-structural element'. Many ways of the EMI interpretation were proposed. One of the most perspective is mathematical simulation of mechanical impedance of structural element. The simple models of the EMI were developed and used for some applications [11-14].

In structural health monitoring (SHM) of aircraft structure that basis on ultrasound non-destructive inspection the concept of electromechanical impedance (EMI) can be effectively used for detection of different types of damages (crack, corrosion, delaminating etc.). The effect of structural damage is associated with the changes of dynamic properties of a structure and they cause evolution of different kinds of dynamic response of system that can be measured and analyzed. One of them is EMI of system 'ultrasound sensor-structural element' at harmonics excitation.

Some problems of the electromechanical impedance (EMI) method for structural health monitoring of aircraft are analyzed in this paper. First of all a lot of experimental data on the effect of different types of damage to the EMI was obtained in special tests on the sample with artificial and natural defects. The stable influence of those damages to parameters of EMI was shown.

The key problem of increase of efficiency of EMI inspection is development of acceptable methods of prediction of effect of damage to the impedance. Many ways of the EMI interpretation were proposed. One of the most perspectives of them to which was focused this

investigation is mathematical simulation of EMI of a system ‘structural element-ultrasonic transducer’.
At both cases the theoretical electromechanical impedance Z can be estimated by formula

$$Z = \frac{1}{i\omega C}\left[1 - k_{31}^2\left(1 - \frac{w_1(l) - w_1(0)}{d_{31}E_3}\right)\right] \quad (1)$$

where k_{31} and d_{31} is the electromechanical coupling factor and coefficient, transverse to electric field E_3 , C is the capacitance of the piezoceramics transducer, ω is the cyclic frequency.
Main effect of global or local stiffness degradation is associated with a range $w_1(l) - w_1(0)$ of relative displacement of tips of ultrasound transducer. It defines the change of natural frequencies and can be estimated by modal analysis of non-damaged and damaged systems. The imaginary part of the electromechanical coupling parameters defines the effect of damping. The some new results of EMI application are discussed in this paper.

2. Experimental study

2.1. The effect of local stiffness of a sheet

Electromechanical impedance of ‘piezoelectric sensor–structural element’ system is closely related to the local stiffness of a structural element and attenuation properties of system. Here are presented some results obtained during experiments on EMI application for thin walled structure near-field damage detection using piezoelectric active wafer sensors.
Two experiments were carried out. The first one involved local sensor stiffness increase by constraining the area adjacent to the sensor with two metal bars hold together with the force F as shown in Fig. 1 (a). Second experiment was aimed on local sensor stiffness decrease by cutting a slit parallel to the sensor as can be seen in Figure 1 (b).

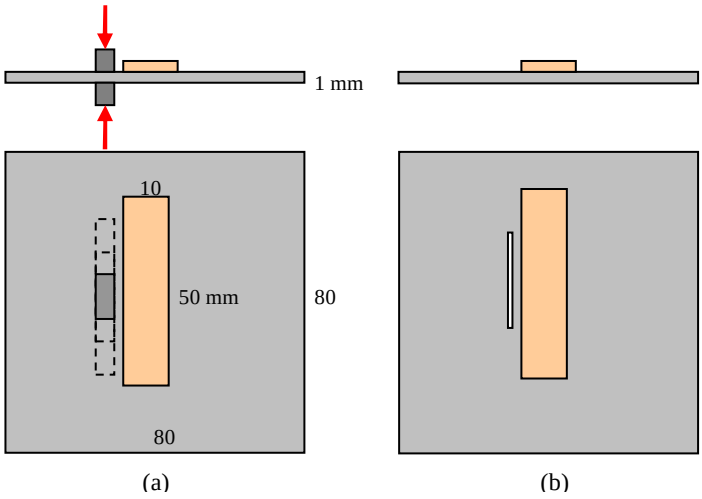

Figure 1. Sensor local stiffness increase (a) and decrease (b) effect on EMI experimental

The PI Ceramic PIC 151 piezoceramic sensor sized 0.5x10x50mm was glued on Al alloy 2024-T3 1x80x80 mm plate. Sensor was bonded to the plate surface with the Epoxy Paste

HYSOL EA 9309. Sensor impedance was measured by the Cypher instruments(c) C60 device. The testing harmonic frequency range was 20-40 kHz and 1024 samples recorded.
The dimensions of constrain steel bars were 10x6, 15x6, 20x6mm. Holding force ***F*** magnitude equalled 500N. The slit size started from 5 to 40mm and was cut from the sensor central axis symmetrically to both sides.
Stiffness variation described changes the impedance resonance frequencies and amplitudes as can be seen in Figure 2 and 3. In the pictures the first resonance band from 32500 to 36500 Hz is shown.

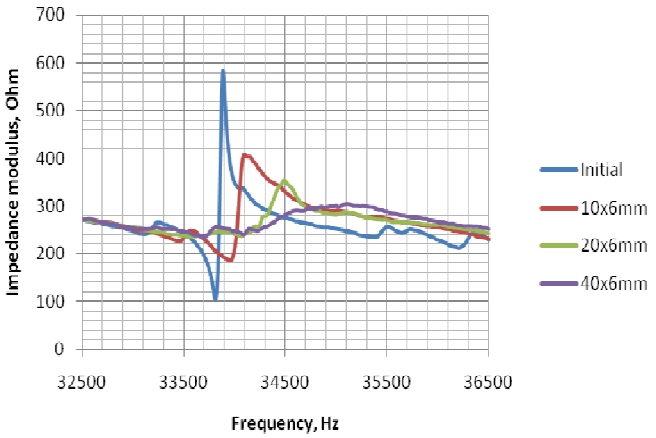

Figure 2. The first resonance of a constrained sensor (local stiffness increase)

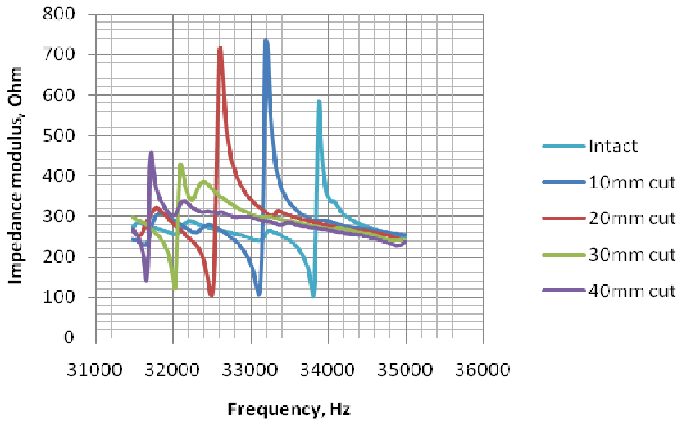

Figure 3. The first resonance of sensor with decreasing local stiffness

For the chosen band the resonance frequency from the damage length can be seen in Figure 4.

As can be seen there is a close correlation between the damage size and resonance frequency.

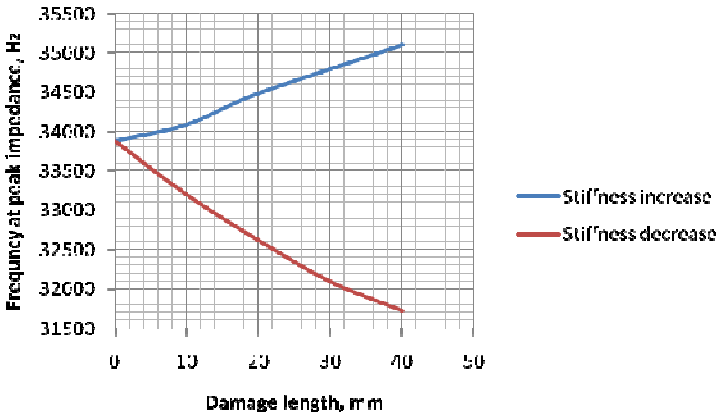

Figure 4. Local stiffness effects on the first resonance frequency

2.2. The effect of holes

Results of measurement are saved in Cypher electronics (C60) files and text files (in folder impedance).

The effect of specific artificial damage of a plate (holes) to EMI was investigated. The system of the 4mm diameter holes were drilled in the 1mm Al2024-T3 sheet 80x150 mm near a PZT PIC 151 1x80x300mm in series of hole's numbering (Figure 5,a). After each drilling the EMI was measured by Cypher electronics C60 instrument.

On the right-hand side of Figure 1 (b) the effect of 4 mm holes near PZT is demonstrated. The smoothed real part of EMI relative increment $\overline{\Delta R}$ in frequency range close to resonance is used as a parameter of holes influence.

$$\overline{\Delta R} = \left| \frac{Re\, Z}{Re\, Z_0} - 1 \right|, \qquad (2)$$

where Z un Z_0 is current and initial electromechanical impedance respectively.

It is seen that parameter monotonically increases in mentioned range of frequency, if a number of holes increases.

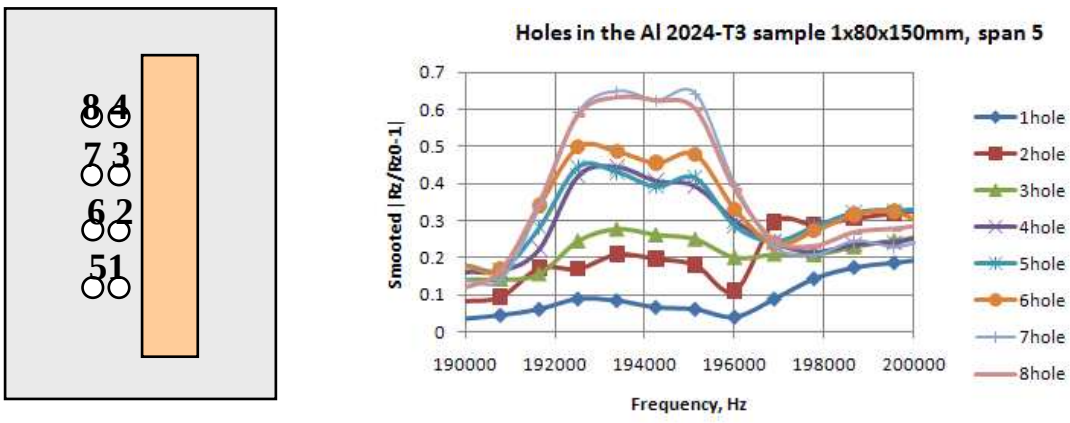

a) b)

Figure 5. The scheme of holes in a plate near PZT (a) and smoothed real part of EMI relative increasing in frequency band near resonance (b)

2.3. Electromechanical impedance for SHM of a bolt-joint

There are many benefits of high preload of bolts. Very important feature of preloaded bolt-joints is the high fatigue strength. Decrease of preload results the decrease of fatigue strength of bolt-joint. Therefore, preload of bolts can serve as the key parameter of technical state of the bolt-joint in the monitoring system. The brief review of recent research in this area is presented in the article [17]. The nuts or washers were equipped by piezo-sensors and 'preload-EMI' correlation was established. The simple theoretical model also was developed.

In Figure 6 the part of the frame 17 of the Mi-8 helicopter tail beam is shown. The main function of this frame is the tail beam joining with the beam of tail propeller. It is realized by a bolt-joint. Three bolts numbered by 1,2,3 are seen in Figure 6. It is seen the pitch of bolts is no uniform here: the distance between ***1*** and ***2*** bolts is more than between ***2*** and ***3*** ones. On the surface of the frame near bolts three piezoceramics transducers Pz 27(InSensor) 6.35x6.35x1 mm were glued by Electrically Conductive Adhesive EPO-TEK EE129-4 and they are numbered by T_1, T_2 and T_3. The bolt-joint was preloaded by creation of the axial force in the bolt shank. This operation was done by a wrench with control of the torque.

The maximal preload in cross-section of a bolt is equal 30 kN that corresponds to stress about 200 MPa.

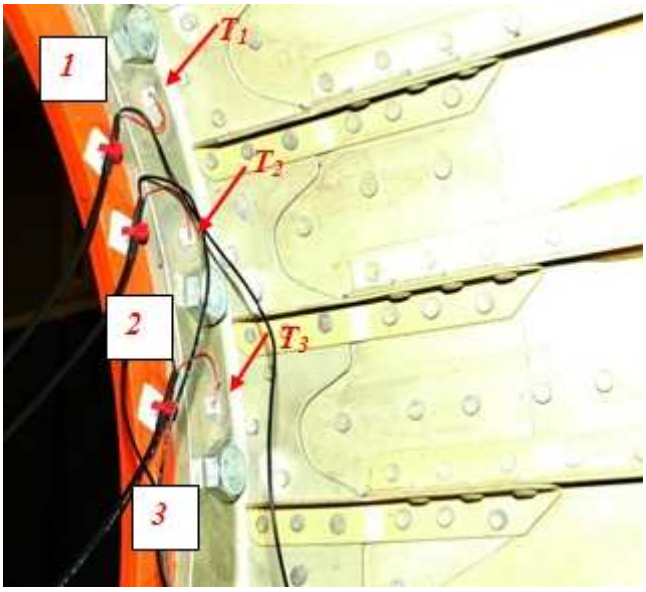

Figure 6. The fragment of the frame 17 of the Mi-8 helicopter tail beam with three piezoceramics transducers near bolts

The program of test contained consequential changes of each bolt preload to 24 and 18 kN (80 and 60% of maximal preload) and EMI measurement of each transducer. The real part relative increment (2) was selected as a parameter for estimation of preload effect.

Results of test is presented in Figures 7-9. It is seen one general tendency: the relative increment of real part of EMI in resonance frequency band increases as a result of loosing of bolt preload. There are presented smoothed function with the span 5. The most significant it is for the nearest transducer from weakened bolt. For example, the maximum of EMI increment of the transducer T_1 is equal 0.0614 and 0.1036 for 80% and 60% of nominal preload (24 and 18 kN). These parameters of others transducers are much less and are not more than 0.03. Similar tendencies are observed for the transducers T_2 and T_3. Easy see also the maximums

for all transducers at 60% of nominal preload are scattered in range 0.1-0.25 that presumably due to the individual properties of sensors and their coupling with the frame.

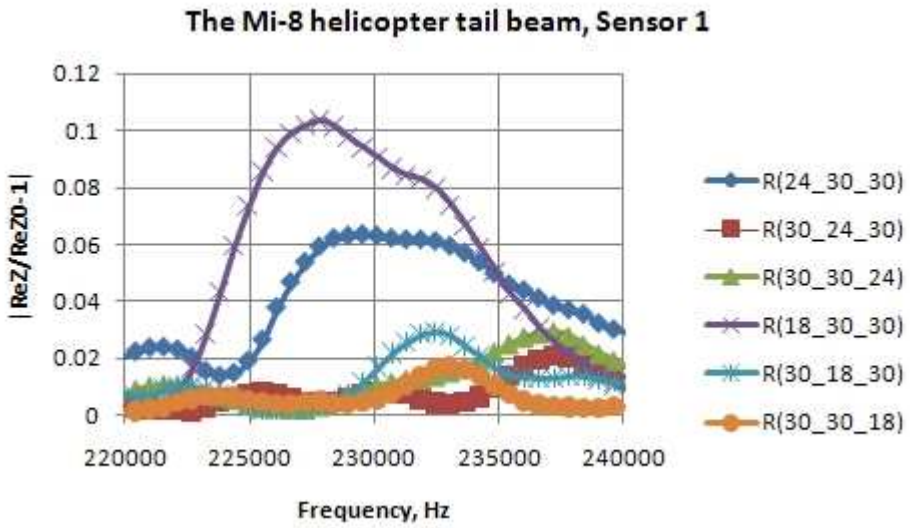

Figure 7. The relative increment of real part of EMI of the transducer T_1 in resonance frequency band as a result of loosing of bolt preload.

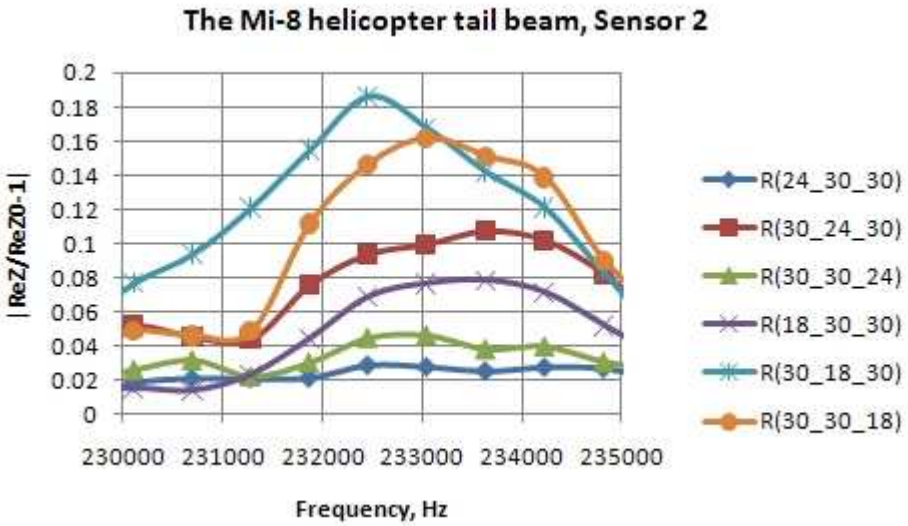

Figure 8. The relative increment of real part of EMI of the transducer T_2 in resonance frequency band as a result of loosing of bolt preload.

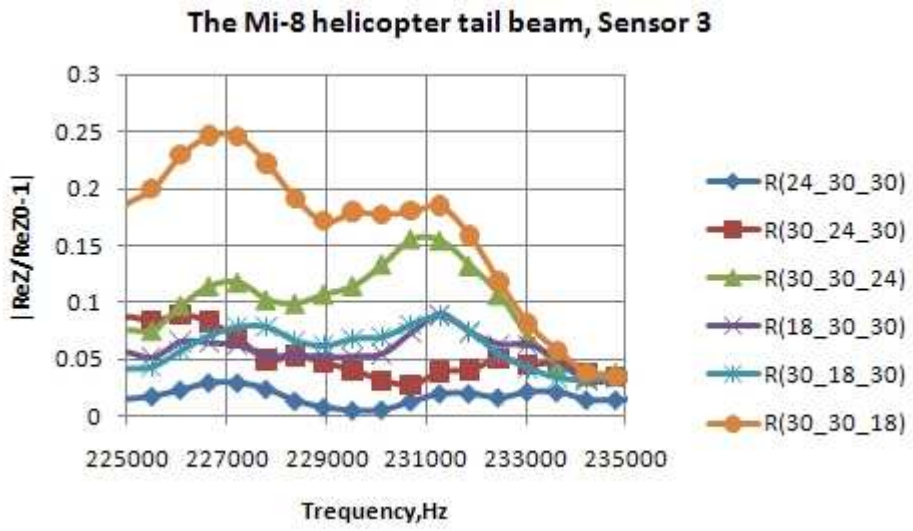

Figure 9. The relative increment of real part of EMI of the transducer T_3 in resonance frequency band as a result of loosing of bolt preload.

3. Analytical study and comparison with test results

3.1. The electromechanical impedance of constrained transducer

If the ultrasound transducer is constrained, the EMI of a system differs from this one in free state. Because the typical damages (crack, corrosion) change the local stiffness of structural element, the EMI of transducer also changes itself.
The 1-D model of constrained piezoceramics transducer (PZT) was developed and described in [13,14]. The simplest type of constrained transducer is shown in Figure 10.

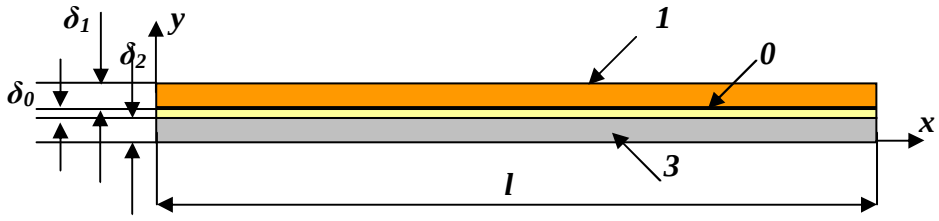

Figure 10. Piezoceramics transducer ***1*** , structural element ***2***, and glue layer ***0***

System of differential equations for the one-dimensional model of elastic wave propagation is:

$$\begin{cases} \dfrac{\partial^2 u_1}{\partial t^2} = c_{1(1)}^2 \dfrac{\partial^2 u_1}{\partial x^2} - \dfrac{c_{1(1)}^2 b_1}{(1+\nu_1)\delta_1 A_1} \dfrac{2G_2\delta_0}{G_0\delta_2 D_0}(u_1 - u_2) \\ \dfrac{\partial^2 u_2}{\partial t^2} = c_{1(2)}^2 \dfrac{\partial^2 u_2}{\partial x^2} + \dfrac{c_{1(2)}^2 b_2}{(1+\nu_2)\delta_2 A_2} \dfrac{2G_1\delta_0}{G_0\delta_1 D_0}(u_1 - u_2) \end{cases} \quad (3)$$

where u_i, ρ_i, E_i, G_i, A_i, b_i, δ_i are axial displacement, density, elastic modulus, shear modulus, cross-section area and its width and thickness for each layer (i=0,1,2).
Solution was accepted in a standard form of two harmonic functions of time:

$$u_1(x,t) = U_1(x)e^{i\omega t},\ u_2(x,t) = U_2(x)e^{i\omega t} \tag{4}$$

Finally the theoretical electromechanical impedance Z can be estimated by formula

$$Z = \frac{1}{i\omega C}\left[1 - k_{31}^2\left(1 - \frac{U_1(l) - U_1(0)}{d_{31}E_3}\right)\right] \tag{5}$$

where k_{31} is the electromechanical coupling factor, transverse to electric field, and $C = \varepsilon_{33}^T \frac{b_1 l}{\delta_1}$ is the capacitance of the piezoceramics transducer, ω is the cyclic frequency.

3.2. General model of EMI of conservative elastic system

The dynamic reaction of an elastic linear system under some external load can be described as a decomposition of displacement vector to the natural functions $\overline{W}_k(x,y,z)$(k=1,…,∞) of linear combination.

$$\overline{w}(x,y,z,t) = \sum_{k=1}^{\infty} \overline{W}_k(x,y,z)\theta_k(t) \tag{6}$$

where $\theta_k(t)$ is so called normal function that is a solution of following ordinary differential equation

$$M_k\ddot{\theta}_k(t) + M_k\omega_k^2\theta_k(t) = \Phi_k(t) \tag{7}$$

Here

$$M_k = \iiint_W \rho(x,y,z)\overline{W}_k^2(x,y,z)dV,\ \Phi_k(t) = \iiint_W \overline{F}(x,y,z,t)\overline{W}_k(x,y,z)dV \tag{8}$$

is a generalized mass of a system and a generalized force respectively associated with k mode of natural oscillation. The natural frequency of this mode is ω_k.
The dynamic reaction $\overline{w}(x,y,z,t)$ at harmonic excitation in surround of natural frequency ω_k is mainly defined by dynamic properties of this mode. It means, if $|\omega_k - \omega| \to 0$, then

$$\overline{w}(x,y,z,t) \to \frac{\Phi_{k0}\overline{W}_k(x,y,z)}{M_k(\omega_k^2 - \omega^2)}e^{i\omega t} \tag{9}$$

where $\Phi_{k0} = \iint_S \overline{Q}(x,y,z)\overline{W}_k(x,y,z)dS$ and $\overline{Q}(x,y,z)$ is an amplitude of the harmonic excitation force. It means that $\overline{F}(x,y,z,t) = \overline{Q}(x,y,z,t)e^{i\omega t}$.

It is the important feature of function $\overline{w}(x,y,z,t)$ that can be effectively used for the EMI approximate estimation. Two views of the system 'structural element-ultrasound transducer' is presented in Figure 11, a.

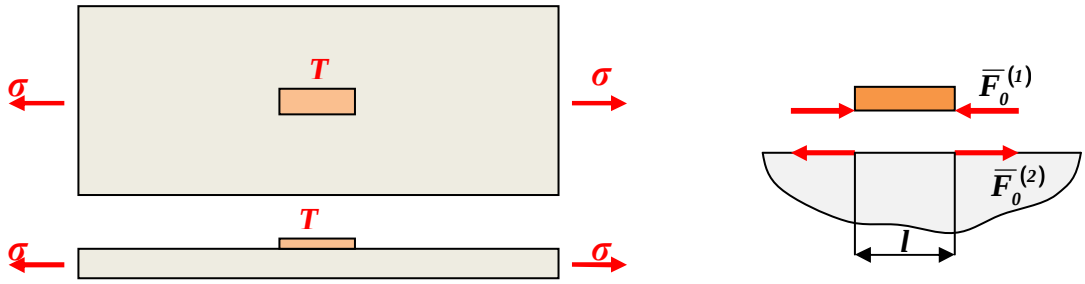

a) b)

Figure 11. The views of the system 'structural element-ultrasound transducer' (a) and the simplified scheme of interaction of a transducer with structural element (b)

The prismatic geometrical shape of a transducer is accepted. It is assumed that the dynamic properties (natural modes and frequencies) both isolated components of this system are known. The dynamic properties of system and finally the amplitude of transducer elongation should be estimated.

$$\frac{\Phi_{k0}^{(1)}\overline{W}_k^{(1)}(x,y,z)}{M_k^{(1)}\left(\omega_{k1}^2-\omega^2\right)}e^{i\omega t}=\frac{\Phi_{m0}^{(2)}\overline{W}_m^{(2)}(x,y,z)}{M_m^{(2)}\left(\omega_{m2}^2-\omega^2\right)}e^{i\omega t} \qquad (10)$$

Here k is number of transducer mode with natural frequency nearest to frequency of forced load, but m is analogical mode of structural element.

If two linearly elastic systems are relatively constrained, then at the natural vibration of the joined system with some natural frequency ω vibration of the each component is forced by harmonic load of the same frequency. Obviously this load is dynamic reaction of other component. Type, distribution and value of this load is defined by internal constrains.

$$\Phi_k^{(i)}(t)=\iint_S \overline{F}^{(i)}(x,y,z,t)\overline{W}_k^{(i)}(x,y,z)dS, \qquad \overline{F}^{(i)}(x,y,z,t)=\overline{F}^{(i)}(x,y,z)e^{i\omega t}$$

$$\Phi_{k0}^{(i)}=\iint_S \overline{F}_0^{(i)}(x,y,z)\overline{W}_k^{(i)}(x,y,z)dS, \quad \Phi_k^{(i)}(t)=\Phi_{k0}^{(i)}e^{i\omega t}, \quad \overline{F}_0^{(1)}(x,y,z)=-\overline{F}_0^{(2)}(x,y,z)$$

If the simplified scheme of interaction of a transducer with structural element is accepted (Figure 11, b), then

$$\Phi_{k0}^{(i)}=\iint_S \overline{F}_0^{(i)}(x,y,z)\overline{W}_k^{(i)}(x,y,z)dS\approx(-1)^i F_0^{(i)}\Delta W_k^{(i)}bl \qquad (11)$$

Here $\Delta W_k^{(i)}$ is the increment of k^{th} natural mode of i^{th} element of system at base l of transducer.

Taking into account the expression (11) the equation (10) can be transformed to following form:

$$-\frac{\left[\Delta W_k^{(1)}\right]^2}{M_k^{(1)}\left(\omega_{k1}^2-\omega^2\right)}=\frac{\left[\Delta W_m^{(2)}\right]^2}{M_m^{(2)}\left(\omega_{m2}^2-\omega^2\right)} \qquad (12)$$

As a result the natural frequency of the system 'structural element-ultrasound transducer' induced by mode k of a transducer and mode m of a structural element cab be estimated by formula

$$\omega^2 = \frac{\left[\Delta W_k^{(1)}\right]^2 M_m^{(2)} \omega_{m2}^2 + \left[\Delta W_m^{(2)}\right]^2 M_k^{(1)} \omega_{k1}^2}{\left[\Delta W_k^{(1)}\right]^2 M_m^{(2)} + \left[\Delta W_m^{(2)}\right]^2 M_k^{(1)}} \tag{13}$$

It means if the natural frequency is used as a parameter of EMI for structural health monitoring, then the formula (13) can be used for theoretical prediction of damage effect.
Similar approach can give an estimate of EMI magnitude and at the combining with concept of complex stiffness it is possible to obtain also an estimate of EMI phase. Below the approximate theory of damage effect to EMI is given.
If the system is loaded by a cyclic force generated by piezo-transducer, then the axial force in the cross-section of transducer can be defined by following way.
Axial strain of a prismatic transducer is

$$S_{11} = s_{11} T_{11} + d_{31} E_3 = S_{11}^* + d_{31} E_3 \ , \tag{14}$$

where S_{11}^* is axial strain induced by axial force F_0 (mechanic part of a strain)in a rectangular cross-section of transducer with the width b and the thickness t, s_{11} is the longitudinal elastic compliance of material of piezo-transducer. The member $d_{31} E_3$ in (14) is piezoelectric part of a strain.
The condition of strain compatibility

$$\Delta w_1 = \Delta w_1^* + d_{31} E_3 l = \Delta w_2 \, , \tag{15}$$

where Δw_1^* is mechanic part of axial increment of displacement, together with asymptotic expression (9) gives equation for interacting axial force F_0 definition:

$$\frac{\left[\Delta W_m^{(2)}\right]^2 F_0}{M_m^{(2)}\left(\omega_{m2}^2 - \omega^2\right)} = -\frac{\left[\Delta W_k^{(1)}\right]^2 F_0}{M_k^{(1)}\left(\omega_{k1}^2 - \omega^2\right)} + d_{31} E_3 l \tag{16}$$

This force is:

$$F_0 = \frac{d_{31} E_3 l}{\left\{ \frac{\left[\Delta W_m^{(2)}\right]^2}{M_m^{(2)}\left(\omega_{m2}^2 - \omega^2\right)} + \frac{\left[\Delta W_k^{(1)}\right]^2}{M_k^{(1)}\left(\omega_{k1}^2 - \omega^2\right)} \right\}} \tag{17}$$

Finally the estimate of axial increment of displacement is expressed by formula:

$$\Delta w_1 = \Delta w_2 \approx \frac{d_{31} E_3 l}{\left\{ \frac{\left[\Delta W_m^{(2)}\right]^2}{M_m^{(2)}\left(\omega_{m2}^2 - \omega^2\right)} + \frac{\left[\Delta W_k^{(1)}\right]^2}{M_k^{(1)}\left(\omega_{k1}^2 - \omega^2\right)} \right\}} \frac{\left[\Delta W_m^{(2)}\right]^2}{M_m^{(2)}\left(\omega_{m2}^2 - \omega^2\right)} \tag{18}$$

As a result, using formulas (1) and (18) the EMI can be approximately expressed by formula

$$Z = \frac{1}{i\omega C}\left\{1 - k_{31}^2\left[1 - \frac{\left[\Delta W_m^{(2)}\right]^2}{\frac{\left[\Delta W_m^{(2)}\right]^2}{M_m^{(2)}\left(\omega_{m2}^2 - \omega^2\right)} + \frac{\left[\Delta W_k^{(1)}\right]^2}{M_k^{(1)}\left(\omega_{k1}^2 - \omega^2\right)}}\right]\right\} \qquad (19)$$

3.3. Example: the thin sheet with a crack

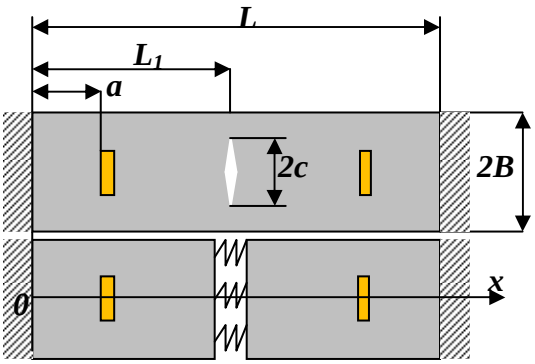

Figure 12. The crack in the thin plate (top) and approximate simulation of its effect to stiffness (bottom)

The simple rectangular plate with the central symmetric crack is considered (Figure 12 top). The vertical sides of a plate are fixed. Two piezoceramics transducers of rectangular shape are glued on the surface of a plate. The dynamics properties and EMI of system ‚plate – transducer' are analyzed.

In the theoretical analysis the effect of a crack is approximately estimated by the increasing of elastic compliance of a plate (Figure 12 bottom) replacing weakens effect of a crack by some equivalent elastic spring (1D model). The estimation of elastic compliance increasing can be executed by the use of the energetic approach of fracture mechanics.

This reception has been successfully used earlier for an estimation of influence of a crack on rod and rod system [3,4].

The principle of the reciprocity works (Maxwell's theorem) is the basis of this concept. It allows to define a compliance of an equivalent elastic spring that causes the increment of integral displacement of a plate as well as the crack. In case of the general crack this additional compliance δ_j corresponded to the generalized force Q_j can be defined by formula:

$$\delta_j = \frac{2}{Q_j^2}\int_S\left[\frac{\left(1-\nu^2\right)}{E}\left(K_I^2 + K_{II}^2\right) + \frac{1+\nu}{E}K_{III}^2\right]dA\,, \qquad (20)$$

where K_I, K_{II}, K_{III} are stress intensity factors of three modes caused by the generalized force Q_j ; E is the module of elasticity and ν is Poisson's ratio; A is area of crack surface. It is assumed that there is the plane strain in a surround of crack front.

In the considered problem the stress intensity factor (SIF) of first mode K_I is non-zero only and in this case there is the plane stress. This SIF can expressed by formula

$$K_I = \frac{F}{A}\sqrt{\pi c}\,\varphi(c/B) = \sigma\sqrt{\pi c}\,\varphi(c/B), \qquad (21)$$

where F is tension force subjected a plate, $\varphi(c/B)$ is the correction function of the sizes and form of a plate with a crack. It was obtained numerically by M.Isida [18] and with can be approximated by polynomial function (difference is less than 0.6%, if $\lambda < 0.6$):

$$\varphi(\lambda) = 1 + 0.0248\lambda + 0.3554\lambda^2 + 0.9063\lambda^3\,, \qquad (22)$$

where $\lambda = \frac{c}{B}$.

If the thickness t of a plate is constant, then the area of crack surface $A = 2tc$ and it is a function of crack half-length c. As a result, the surface integral in (20)

$$\delta = \frac{4t}{F^2 EA^2}\int_0^c K_I^2 dc = \frac{4\pi B^2}{EA^2}\int_0^c \lambda\varphi^2(\lambda)d\lambda = \frac{2\pi B}{EA}\int_0^{c/B} \lambda\varphi^2(\lambda)d\lambda \qquad (23)$$

Relative additional compliance caused by a crack is:

$$\bar{\delta} = \frac{\delta}{\delta_0} = \frac{2\pi B}{L}\int_0^{c/B} \lambda\varphi^2(\lambda)d\lambda, \qquad (24)$$

where $\delta_0 = \frac{L}{EA}$ is the tensile compliance of the non-cracked plate.

Using expression (24), the relative additional compliance as a function of crack half-length was obtained and presented in Figure 13.

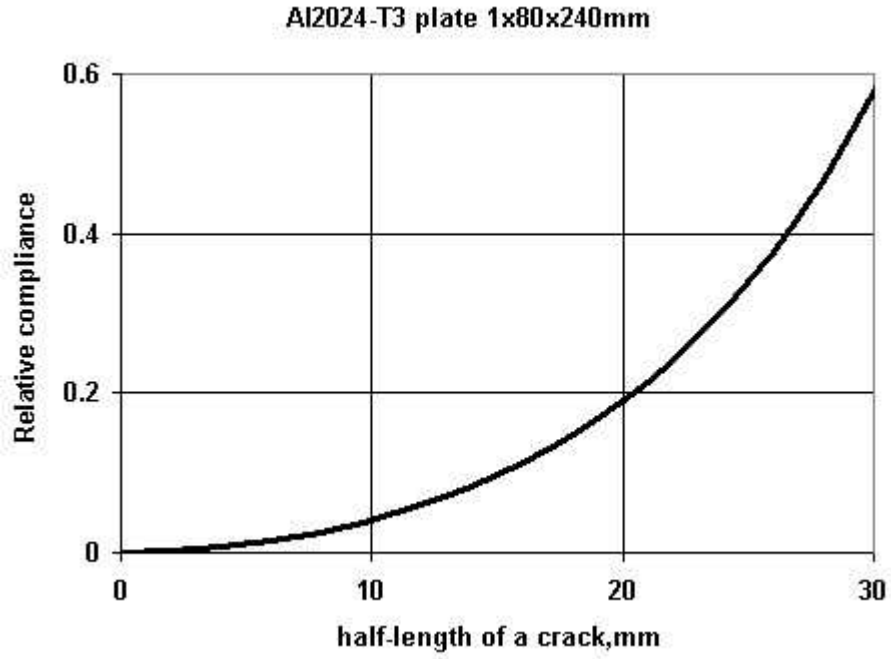

Figure 13. The relative additional compliance of plate as a function of crack half-length

Now the approximate frequency analysis of mentioned system ‚plate – transducer' can be executed. The modal properties of both isolated components of system are needed. For free transducer it is necessary to define only first mode because it provides the most effective possibility to generate Lamb wave [11]. It means that first natural frequency of transducer in longitudinal direction of the plate (look at the Figure 12) is

$$\omega_1^{(1)} = \frac{\pi}{b}\sqrt{\frac{E_1}{\rho_1}}, \qquad (24)$$

where E_1 and ρ_1 is module of elasticity and density of transducer material respectively, b is the width of transducer (a size to direction of axis x).

First mode is $W_1^{(1)}(x) = \cos\frac{\pi x}{b}$ and the increment of this function at base b is:

$$\Delta W_1^{(1)}\Big|_b = \cos\frac{\pi x}{b}\Big|_0^b = -2 \tag{25}$$

Generalized mass that corresponds to this mode is:

$$M_1^{(1)} = \int_0^b \rho_1 lt \cos^2\frac{\pi x}{b}dx = \frac{\rho_1 btl}{2} \tag{26}$$

For second component (the plate) the natural frequencies can be defined from following the frequency equation:

$$\begin{aligned}&\left[\sin(kL_1) + \bar{\delta}kL\cos(kL_1)\right]\left[\sin kL\sin(kL_1) + \cos(kL_1)\cos kL\right] + \\ &+ \cos(kL_1)\left[\sin kL\cos(kL_1) - \sin(kL_1)\cos kL\right] = 0\end{aligned} \tag{27}$$

Here $\bar{\delta} = \frac{\delta}{L/(EA)}$ is relative compliance of the equivalent spring.

It is a transcendent equation and its roots should be defined by numerical method.

The mode m of natural oscillation is:

$$W_m^{(2)}(x) = \begin{cases} C_2 \sin k_m x, & \text{if} \quad x < \frac{L}{2} \\ C_3 \cos k_m x + \sin k_m x, & \text{if} \quad x > \frac{L}{2} \end{cases} \tag{28}$$

where $C_2 = \tan k_m L \cdot \tan k_m L_1 + 1$, $C_3 = -\tan k_m L$.

As a result

$$\Delta W_m^{(2)}\Big|_l = C_2 \sin k_m x\Big|_{x_1}^{x_2} = C_2\left(\sin k_m x_2 - \sin k_m x_1\right), \tag{29}$$

where $x_1 = a$, $x_2 = a + b$.

In the numerical analysis the sizes of a plate and a condition of its supporting have been accepted the same ones as in experiment: 1x80x240мм, material of a plate is the aluminium alloy 2024-T3. There was accepted that along the short edges the plate was motionlessly fixed that corresponds to constrained effect of clamps of the test machine. The longitudinal edges are free from external forces and any constrains. The longitudinal free oscillations of such structure were analyzed.

Figure 14 presents some results of the analysis. Plot of ten natural frequencies as functions of half-length of a crack is shown. It is seen for modes of oscillation at which the unit line of the mode coincides with an axis of a crack, frequency of natural oscillation does not vary. For symmetric modes the increase in length of a crack causes decrease in frequency of natural oscillation.

First natural frequency of a free transducer (FFT): 146.2 kHz

It means that the EMI of system related with damage of a sheet can be observed in the frequency band 100-200 kHz.

The closest natural frequency of a plate at non-damaged state less than FFT is equal to 134.3 kHz and corresponds to 4th mode of a sheet. The closest natural frequency of a plate at non-damaged state more than FFT and affected by crack growth is equal to 167.8 kHz and corresponds to 5th mode of a sheet. The crack in the middle cross-section of a plate does not affect to frequency of 5th mode. Therefore the natural frequency of a system generated by interaction with this mode is independent from mentioned damage and is non-informative for

its detection. The next natural frequency of a plate at non-damaged state more than FFT and affected by crack growth is equal to 201.4 kHz and corresponds to 6th mode of a sheet.
The numerical analysis using (13) and the estimates of dynamic properties of components gave the estimates of natural frequencies of a system in narrow band close to first natural frequency of a transducer. As it should suppose the natural frequencies of a system practically coincide with they of a plate.

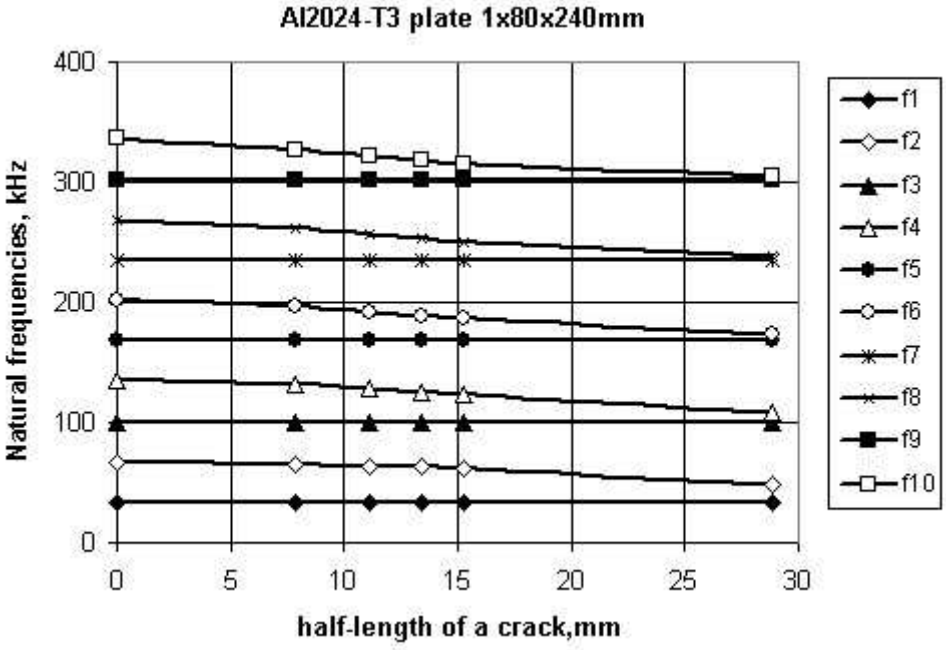

Figure 14. The natural frequencies of the plate as functions of half-length of a crack

3.4. Comparison with test results

Impedance of the piezoceramics transducer PIC151 0.5x10x50 mm installed to surface of the Al sample described above was measured during fatigue test at the stage of crack growing. The impedance measurement device C60 of Cypher was used in frequency band 10 kHz-1MHz. Some results are presented in Figure 15, 16 and 17. Three resonance frequencies were observed in frequency band 80-200 kHz. First of them was fixed in range 82-88 kHz (Figure 15). It is seen the resonance frequency corresponded to minimum of EMI magnitude has a tendency of decreasing, if fatigue crack length increases. Second and third resonance frequencies in range 134-140 kHz (Figure 16) and 170-180 kHz (Figure 17) respectively have the same tendency of changing as a function of the crack length.
It can be concluded that the estimated frequency and trends of EMI qualitatively consistent with the results obtained in the experiment. However, there are significant deviations from the prediction. First of all, experimentally defined frequencies are slightly lower in comparison with the theory. Mainly this is due to the proximity of the one-dimensional model of a plate with damage (crack), as well as with the idealization of conditions. FEA shows that even flat natural modes significantly more complex and their number is a lot more than is predicted by the one-dimensional model. Although the frequencies of the appropriate modes are close enough to theory. Especially the elastic compliance of supports can greatly affect the modal characteristics of elastic system, as shown, for example, in [19]. A significant factor is the

attenuation of ultrasonic signal at its propagation. The developed model is not taken into account the effect of this factor.

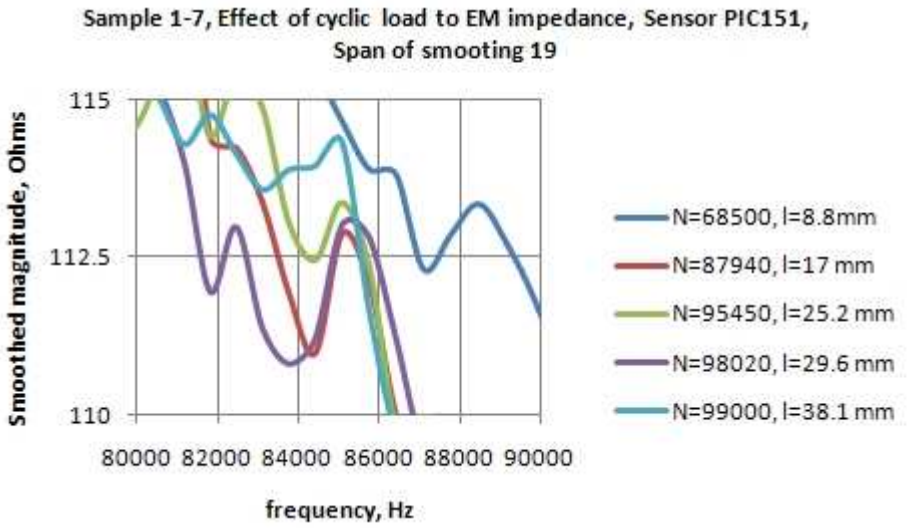

Figure 15. Magnitude of EMI of system in narrow frequency band lower than the first natural frequency of transducer

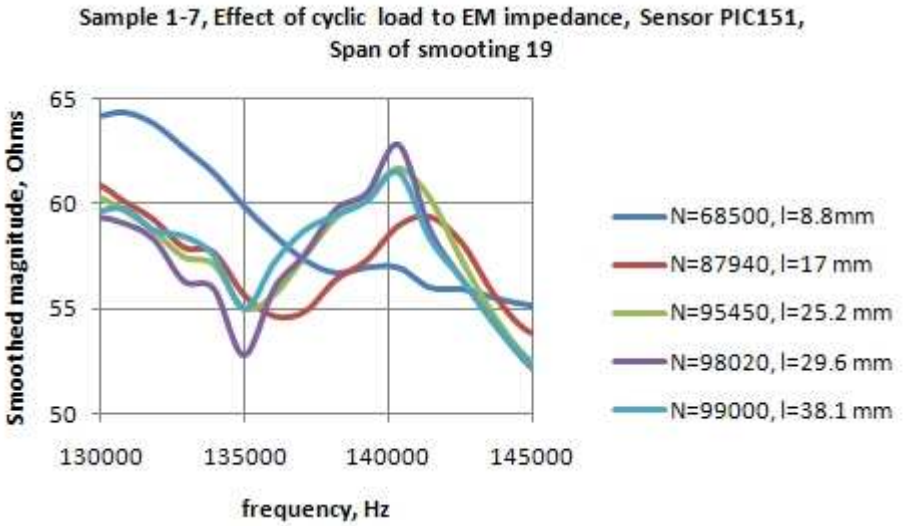

Figure 16. Magnitude of EMI of system in narrow frequency band close to the first natural frequency of transducer

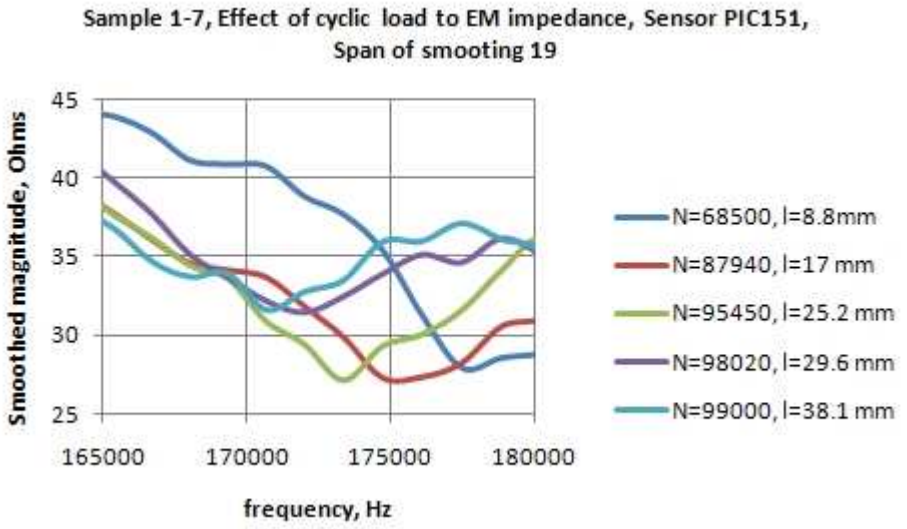

Figure 17. Magnitude of EMI of system in narrow frequency band higher than the first natural frequency of transducer

4. Conclusions

The effect of structural damage is associated with the changes of dynamic properties of a structure and can be effectively defined at ultrasonic frequencies by identification of EMI of system 'sensor-structural element'. The developed 1-D model of constrained PZT can be used for analysis of the elastic and geometrical parameters effect to properties of piezoceramics transducer, and for structural health monitoring of element with possible damage.
The key problem of increase of efficiency of EMI inspection is development of acceptable methods of prediction of effect of damage to the impedance. The simple method of estimation was developed. This method uses the effect of natural frequency changing as a result of PZT and structural element coupling. The effect of a crack is approximately estimated as a function of elastic compliance of a plate using the energetic approach of fracture mechanics. The model of constrained piezoceramics transducer can be also used for creation of a type of pre-stressed one protected from effect of mechanical fatigue and environmental degradation.

Acknowledgement. The research leading to these results has received funding from the European Community's Seventh Framework Program [FP7/2007-2013] under grant agreement n°212912. The authors are grateful to European Commission for financial support and all partners for scientific and technological collaboration.

References

1. Liang, C., Sun, F.P. and Rogers, C.A. Coupled electro-mechanical analysis of adaptive material system-determination of the actuator power consumption and system energy transfer. Journal of Intelligent Material Systems and Structures, 5, pp.12–20, 1994.
2. Sun, F.P., Liang, C. and Rogers, C.A. Experimental modal testing using piezoceramic patches as collocated sensors-actuators. Proceeding of the 1994 SEM Spring Conference and Exhibits, Baltimore, MI, June 6–8, 1994.

3. Sun, F.P., Chaudhry, Z., Rogers, C.A. and Majmundar, M. Automated real-time structure health monitoring via signature pattern recognition. Proceedings, SPIE North American Conference on Smart Structures and Materials, Vol. 2443 . San Diego, CA, 26 Feb.–3 March, pp. 236–247, 1995.
4. Chaudhry, Z., Sun, F.P. and Rogers, C.A. Health monitoring of space structures using impedance measurements. Fifth International Conference on Adaptive Structures, Sendai, Japan, 5–7 December, pp. 584–591, 1994.
5. Chaudhry, Z., Joseph, T., Sun, F. and Rogers, C. Local-area health monitoring of aircraft via piezoelectric actuator/sensor patches. Proceedings, SPIE North American Conference on Smart Structures and Materials, Vol. 2443 . San Diego, CA, 26 Feb.–3 March., pp. 268–276, 1995.
6. Ayres, T., Chaudhry, Z. and Rogers, C. Localized health monitoring of civil infrastructure via piezoelectric actuator/sensor patches. Proceedings, SPIE's 1996 Symposium on Smart Structures and Integrated Systems, SPIE, Vol. 2719, pp. 123–131, 1996.
7. Giurgiutiu, V. and Rogers, C.A. Electro-mechanical (E/M) impedance method for structural health monitoring an non-destructive evaluation. Int. Workshopon Structural Health Monitoring Stanford University, CA, 18–20, pp. 433–444, September 1997.
8. Giurgiutiu, V. and Zagrai, A. Characterization of piezoelectric wafer active sensors. Journal of Intelligent Material Systems and Structures, 11(12), pp.959–976, 2000.
9. Giurgiutiu, V., Zagrai, A. and Bao, J. (2002). Piezoelectric wafer active sensors (PWAS), USC IPMO Invention Disclosure #00330/2002.
10. Victor Giurgiutiu, Andrei Zagrai and Jing Jing Bao. Piezoelectric Wafer Embedded Active Sensors for Aging Aircraft Structural Health Monitoring. SHM, 2002, Vol 1(1): 0041–61
11. Giurgiutiu, V. Structural Health Monitoring with Piezoelectric Wafer Active Sensors, Elsevier Academic Press, 2008, 760 pages.
12. Adams D.E. Health Monitoring of Structural Materials and Components: Methods with Application, John Wiley & Sons, Ltd. (2007), 460 pp.
13. I.Pavelko. Research on the Protection of Piezoceramics Transducers from the Destruction by Mechanical Loading. Int.Virtual J. for Science, Technics and Innovations for the Industry, Issue 7, pp.17-21, 2010.
14. I.Pavelko, V.Pavelko, S.Kuznetsov, E.Ozolinsh, I.Ozolinsh, H.Pfeiffer, M.Wevers. Problems of structural health monitoring of aircraft component. The proceeding of 27th Congress of the International Council of the Aeronautical Sciences, Nice, France, 19-24 September 2010, (Section 10, ICAS 2010-10.6.1).
15. I.Pavelko, V.Pavelko. The valuation of stiffness of rods with cracks. – "Tarptautines konferencijos pranesimus medziaga Transporto priemones – 97". Kaunas: Technologija, pp.237 – 241, 1997.
16. I.Pavelko, V. Pavelko. Calculation of bar systems with crack by a finite element method// Scientific proceeding of Riga Technical University: Transport end Engineering. Mechanics, Volume 6, Number 7. – Riga: RTU, pp.159-163, 2002.
17. D. L. Mascarenas, G. Park∗, K.M. Farinholt, M.D. Todd, and C.R. Farrar. A low-power wireless sensing device for remote inspection of bolted joints. Proc. IMechE Vol. 223 Part G: J. Aerospace Engineering, pp.565-575, 2009.
18. M. Isida. Proc**.** 4th U.S.Nacional Congress of Applied Mechanics, pp.955-970, 1966.
19. Igor Pavelko, Vitalijs Pavelko. Dynamic properties of aircraft components at real constraints. Vilnius Gediminas Technical University. AVIATION, vol. 12. no. 4. Vilnius TECHNIKA, pp. 113-117 , 2008.